

pubs.acs.org/Macromolecules Article

Dynamics across a Free Surface Reflect Interplay between Density and Cooperative Length: Application to Polystyrene

Ronald P. White and Jane E. G. Lipson*



Cite This: Macromolecules 2021, 54, 4136-4144



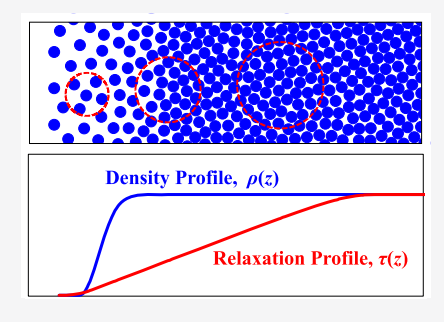
ACCESS I

Metrics & More

Article Recommendations

Supporting Information

ABSTRACT: It is now generally agreed that the most dramatic influence of a free surface on local relaxation dynamics occurs over the first 10 nm from the surface. Using the cooperative free volume (CFV) rate model, we have linked a faster dynamic response to a lower density (i.e., greater available or free volume) closer to the interface. Experimental and simulation studies have shown that the relaxation profile is significantly broader than the local density profile. Here, we explain this difference using the CFV model to show that local relaxation can be enabled through accrual of a fixed amount of free volume, the value of which is a characteristic, material-dependent quantity. The process by which a relaxing segment acquires this volume involves a cooperative region whose length scale will change with density and therefore with distance from the interface. The result is a region-averaged position-dependent density profile that is significantly broadened and



that links directly to the relaxation profile. Finally, we explain why these film confinement effects diminish in importance as the temperature is increased.

1. INTRODUCTION

The effect of interfaces on the structural dynamics of polymers and other glass-forming materials has been of strong interest in experiments, theories, and simulations. 1-12 Some approaches yield results that show how an interface changes properties as averaged over the whole sample, while other more detailed methods track position-dependent dynamics on the nanometer scale. In a recent work $^{13-15}$ with the cooperative free volume (CFV) rate model, $^{16-18}$ we used an overall density value averaged over both outer and inner layers to predict the segmental relaxation times (τ) of polymer films as a whole sample. In this paper, we use the CFV model, but our focus is not on the sample average; instead, we turn to more detailed predictions for τ as a function of position across the interface and focus on changes in the segmental relaxation dynamics to depths of about 5 nm. The CFV model allows us to make a direct connection between density and the relevant length scale over which cooperative motion is required in order for molecular relaxation to occur. Our sample set of calculations is for a polystyrene (PS) free surface, and we conclude by connecting these predictions to experimental and simulation results from the literature.

In models for bulk dynamics such as ${\rm CFV}^{13,16-18}$ and density scaling, $^{19-25}$ the goal is to describe segmental relaxation times, $\tau(T,V)$, as a function of two independent variables, temperature (T) and volume (V). The ability to separate and distinguish the independent volume (density) contribution from that of temperature can lead to significantly more physical insight compared to treating only $\tau(T)$ along a single (ambient) isobar. For example, a film and its corresponding bulk can be at the same temperature and have

different relaxation times; what differentiates the two is their

The connection between confinement and density (or pressure) effects has been featured in a number of studies on polymer films and polymers and small molecules in nanopores. 13-15,26-36 While most of the results from these works strongly support the connection, direct measurement of the density itself is challenging for confined systems.^{37–39} Positron annihilation lifetime spectroscopy (PALS) data analyses^{26,27,33} have verified that there is a difference in the effective density (free volume) for systems confined in nanopores. Further evidence comes from back-calculated specific volumes for (isobaric) films, which show the same coefficient of thermal expansion as the corresponding bulk but have densities that are shifted by ~1-2%. 14 Faster dynamics in supported polymer films 14,29,34 may be promoted by free space near the substrate created from inefficient packing of polymer chains following spin coating; the presence of this additional space has been verified via probe adsorption measurements. 40,41 Large pockets of free space near asperities on rough substrates (analyzed via atomic force microscopy) can also lead to faster dynamics.³¹ Connections with simulation data can also be useful because they can provide very detailed information on local density

Received: December 14, 2020 Revised: March 20, 2021 Published: April 27, 2021





profiles and corresponding dynamics. We will make such comparisons below, where we discuss in detail how our model results for the position-dependent density lead to predictions for cooperative dynamics in an inhomogeneous free surface environment.

Our general form for pressure-dependent dynamics behavior is $\tau(T,V) \propto \exp[f(T) \times g(V)]$, where a key feature is how the temperature and density contributions are multiplicatively coupled. 15 From this fundamental relationship, a general power law form can be derived for isobars, $\tau_2(T) \propto \tau_1(T)^c$, where the exponent $c = g(V_2(T))/g(V_1(T)) = V_{\text{free}1}(T)/V_{\text{free}2}(T)$ (V_{free} defined below) relates to the density dependence and is an approximate constant. This form effectively describes the experimentally observed behavior when "1" and "2" are two isobars of the bulk material, for example, high P and low P. It equally applies to analogous isobars of a polymer film and of its corresponding bulk (e.g., both at ambient P), ¹⁵ an observation first reported by Diaz-Vela et al. 42 Part of the success in our model is due to the fact that the functional form of the temperature-dependent contribution, f(T), is the same for both film and bulk, that is, $f_1(T) = f_2(T) = f(T)$ (we will come back to this point below). The multiplicative coupling in $\tau(T,V) \propto$ $\exp[f(T) \times g(V)]$ also explains why relaxation times for a material at low temperatures become very sensitive to density changes arising from a pressure difference or a difference in film thickness (i.e., why sensitivity to confinement increases at

Confinement effects are often interpreted in terms of how the activation energy ($\Delta A_{\rm act}$) for a local motion is altered by the presence of the interface. Our CFV model for relaxation in a bulk sample links density to the degree of cooperativity, n^* , the number of cooperating segments needed to effect the local motion. We show that this connection follows the form $\Delta A_{
m act}$ $\propto n^* \propto 1/V_{\rm free}$ where $V_{\rm free}$ is the system's free volume above the close-packed state, a very simple function of density. References 16 43, and 44 demonstrate the strength of this predicted correlation using experimental dynamics results along with V_{free} determined from PVT data. At this point, we have analyzed a wide variety of systems, all of which show strikingly linear log τ versus $1/V_{\rm free}$ isotherms with Tdependent slopes. This new connection between the alpha relaxation times and $V_{\rm free}$ explains how $V_{\rm free}(T)$ dictates $\Delta A_{\rm act}(T)$ in driving non-Arrhenius behavior as T decreases along isobars. 18 More connections between free volume, cooperativity, and activation energy have been highlighted in several recent experimental studies employing PALS and dielectric spectroscopy by Araujo et al.45 and Kipnusu et

In addition to CFV, a number of other models have been applied to study the dynamics of confined systems; several examples can be found in the articles and reviews in refs. ^{1,6,7,32,34,47,51} In the following, we give a brief survey of a selection of these approaches and discuss their similarities and differences with CFV.

The ECNLE model^{6,50,52} of Schweizer and co-workers is a detailed pair correlation-based approach that maps an experimental system on to a corresponding hard sphere fluid (e.g., such as to match the experimental compressibility with that of the hard sphere fluid at each given temperature), and from this information, free energy barriers for particle motion can be computed. To model free-standing films, Phan and Schwiezer⁵⁰ implemented ECNLE with a step function density profile, that is, going from bulk to zero density at the free

surface. While the theory-based density profile we use here is not infinitely steep, it is much steeper than the broader relaxation profile which is ultimately found by both approaches. ECNLE is significantly more technically detailed than the CFV, but both involve thermally activated models that involve density and compressibility dependence of the activation barriers.

Salez et al. 49,53 introduced a model for dynamics based on cooperative groups of segments in the form of strings, where the degree of cooperativity is based on the available volume and where the reservoir of available free volume at a free interface will thus be able to influence (reduce) the size of the strings (those that contact it) and thus enhance the dynamics. In describing relaxation times, the T-dependent form for the number of cooperating segments involves the system's ambient density at temperature, T, and its density at T_V which is an assumed kinetic arrest point; the result is the standard VFT form, ^{54–56} ln $\tau \sim 1/(T-T_V)$. This aligns the model with other free volume models ^{57,58} based on the historical Doolittle equation.⁵⁹ It therefore maintains a picture where the dynamics are assumed to depend on free volume alone and where the free volume itself (via the crucial parameter, $T_{\rm V}$) needs to be defined by dynamics data rather than volumetric data. Making the Doolittle assumption inevitably causes a failure to describe pressure-dependent dynamics, $\tau(T,V)$. Because T and V each make independent contributions to dynamics, ^{19,20} the effect due purely to a volume change (upon which the Salez et al. model cooperativity depends) will not be captured. One crucial difference between the CFV model, which captures dynamics data across a wide range of T and P conditions, and Doolittle-based free volume models is that the CFV free volume is not treated as a fitting parameter or function but is predicted using thermodynamic data alone.

Another approach that has been applied to dynamics of bulk and confined systems is that of Long, Merabia, and coworkers. 47,48,60-62 This methodology describes the distribution of relaxation times in terms of free volume, density, and its fluctuations, using a thermodynamic treatment for density and bulk compressibility as a function of T and P. With regard to dynamics, the formulations work explicitly in density. The authors introduce a quantity called the "dynamical free volume", defined using a parameter that is the hypothetical close-packed density at which the relaxation time would diverge. Considering the effects of pressure on dynamics, they link both T and V effects to local density fluctuations, 61 which dictate a facilitation mechanism in heterogeneous relaxation. Instead of modeling a local process that involves activation barriers, as the CFV does, they incorporate the T dependence of density fluctuations to explain the T-based contribution to dynamics at constant volume. With regard to film modeling in particular, the approach of Long and Lequeux⁴⁷ and Merabia et al.,48 as well as that of Lipson and Milner,51 all rely on a heterogeneous picture of the overall sample and characterize the percolation of dense subunits to determine relaxation times (and T_g). For example, Merabia et al.⁴⁸ predict a slowdown (speed up) in dynamics as a consequence of the percolation mechanism being affected by the strengthening (weakening) of a surface interaction parameter. In contrast, the present CFV model focuses on local relaxation as an activated process occurring in the context of a local density that represents the average around the position of interest.

Finally, we note the density scaling approach. ^{19–25,32,34} In density scaling, pressure-dependent dynamics, $\tau(T,V)$, of the

bulk material are expressed in terms of the variable, TV', where γ is a parameter that connects experimental systems to a corresponding simple inverse power law fluid, for which thermodynamic and dynamic properties can be conveniently described. Density scaling formulations yield $\tau(T,V) \propto \exp[A^\phi/(TV')^\phi]$ (A and ϕ are constant parameters), and so like CFV, they result in the general $\tau(T,V) \propto \exp[f(T) \times g(V)]$ form noted above. As with CFV, the presence of an interface produces an effect that is similar to that of changing volume in a bulk system, which means that the f(T) function can be determined from the bulk material and then applied to describe the effects of confinement. Examples of this approach applied to polymer films and small molecules in nanopores are described by Adrjanowicz et al. 32,34

2. CFV MODEL AND APPLICATION TO BULK POLYSTYRENE

The CFV film model results from our previous works ^{13–15,30} make use of a sample-averaged characterization, both for the bulk and for film samples of varying thickness. We now turn to outlining our new free volume-based approach for position-dependent dynamics at interfaces, but begin this description by reviewing the basic CFV model framework for bulk and applying it to PS.

The CFV approach^{16,17} is a rate model based on a cooperative picture where the total activation free energy, $\Delta A_{\rm act} = n^* \Delta a$, changes with the number, n^* , of cooperating segments. In CFV, n^* is determined by the system's free volume, defined through

$$V_{\text{free}} = V - V_{\text{hc}} \tag{1}$$

where V is the system's total volume and $V_{\rm hc}$ is its characteristic limiting hard-core volume at close packing. $V_{\rm hc}$ is a material-specific constant that is determined by analysis of thermodynamic (PVT) data using the locally correlated lattice (LCL) equation of state. The CFV picture is based on the assumption that a critical free volume (v^*) is required for local segmental rearrangement. Dividing v^* by the free volume per segment therefore quantifies the number of cooperating segments, $n^* = v^*/(V_{\rm free}/N)$. This concept of a constant critical free volume will be key in dictating how the cooperative distance changes with position near the interface.

Applying $\Delta A_{\rm act} = n^* \Delta a$ in the Boltzmann factor, where rate $\propto 1/\tau \propto \exp[-\Delta A_{\rm act}/T]$ (and ignoring the gas kinetic $T^{1/2}$ prefactor), leads to the general form noted above

$$\tau = \tau_{\text{ref}} \exp \left[n^* \times \left(\frac{\Delta a(T)}{T} \right) \right] = \tau_{\text{ref}} \exp \left[\left(\frac{1}{V_{\text{free}}} \right) \times f(T) \right]$$
(2)

The form predicts the multiplicative coupling of T, V contributions, that is, $\tau(T,V) \propto \exp[g(V) \times f(T)]$. The free energy of activation per cooperating segment, $\Delta a(T)$, is an unknown function of T, but it is independent of volume. In practice, an empirical T-dependent form $f(T) \sim \Delta a(T)/T \sim 1/T^b$ is applied, where the material-specific scaling exponent D is roughly analogous to the scaling of D in density scaling approaches. The main CFV working expression is therefore

$$\ln \tau = \left(\frac{V_{\text{hc}}}{V_{\text{free}}}\right) \left(\frac{T^*}{T}\right)^b + \ln \tau_{\text{ref}}$$
(3)

Three of the material specific parameters, b, T^* , and $\tau_{\rm ref}$ are determined from the bulk system dynamics data; alternatively, b can be determined from $T_{\rm g}(P)$ from PVT data. On the other hand, $V_{\rm hc}$ and thus all the values for $V_{\rm free}(T,P)=V(T,P)-V_{\rm hc}$ are determined independent of dynamic data via a priori analysis of thermodynamic (PVT) data. Equation 3 is very effective in fitting and predicting experimental relaxation times under general pressure-dependent conditions, that is, $\tau(T,P)$ or equivalently $\tau(T,V)$, for both polymer and small molecule liquids; ref 16 shows a number of examples. For application here to polystyrene (PS), LCL EOS analysis of PVT data size gives $V_{\rm hc}=0.8718$ mL/g. Fitting eq 3 to bulk dynamics data gives $v_{\rm hc}=0.8718$ mL/g. Fitting eq 3 to bulk dynamics data for the LCL and CFV model analyses of bulk PS are available in the Supporting Information.

3. CFV MODEL FOR POSITION-DEPENDENT DYNAMICS AT INTERFACES

In order to model temperature- and position (z)-dependent relaxation times, $\tau(T,z)$, we need to evaluate the position-dependent relative free volume, $(V_{\rm free}/V_{\rm hc})(z)$, at z and then use this as the input in eq 3 to obtain $\tau(T,z)$. One of the key model assumptions is that the temperature-dependent contribution to the dynamics, $f(T) \sim T^*/T^b$, at any position near the interface is the same as that for the bulk material. This allows us to apply $(V_{\rm free}/V_{\rm hc})(z)$ inside eq 3 using the same parameters, b, T^* , $\tau_{\rm ref}$ that were determined above from the bulk material characterization.

The assumption that the bulk f(T) is also applicable in confined systems is supported by the fact that both film and bulk results follow the $\tau_2(T) \propto \tau_1(T)^c$ power law form. Further evidence comes from experimental tests of our whole sample-averaged model for films. In that case, the bulk functional form f(T) was applied using a sample-average value as an input for $(V_{\text{free}}/V_{\text{hc}})(h)$, taking into account the contributions from interior bulk material as well as an interfacial layer, to give $\tau(T,h)$ for films of thickness, h. As noted above, in the work by Adrjanowicz et al., 32,34 polymer films and small molecules in nanopores were modeled using the density scaling approach which also carries the fundamental $\tau(T,V) \propto \exp[g(V) \times f(T)]$ form, and so this means that their bulk f(T) had also proved sufficient.

The reason density correlates with dynamics in the bulk is because it characterizes the intermolecular environment, that is, the crowding from near neighbors, next near neighbors, and so forth. The value of the local density, $\rho(z)$, at just a single point near a free surface does not contain enough information about the intermolecular environment at z because of how rapidly $\rho(z)$ can change with z in an inhomogeneous environment. Therefore, the density (and corresponding free volume) that is relevant for cooperative dynamics near a free surface needs to be carefully considered.

For a given position, z, we define $\rho_{\rm av}(z)$, the average local density, so as to reflect the mechanistic cooperativity associated with local segmental relaxation. This means that $\rho_{\rm av}(z)$ must be an average that captures contributions over distances from z that are on the scale of the size of the region around it that contains cooperating segments. Note that the size of the cooperative region must be at least the size of the intermolecular segmental distance. Because of this, while $\rho_{\rm av}(z)$ will depend on the local density, $\rho(z)$, its profile will extend deeper into the bulk. $\rho_{\rm av}(z)$ is written as

$$\rho_{\rm av}(z) = \frac{1}{V_{\rm coop}(z)} \int \rho(z') dx' dy' dz'$$
(4)

ho(z) and $ho_{\rm av}(z)$ depend only on z, the position in the direction normal to the interface. The integration (average) is carried out over the values of x', y', z' that are within a cooperative region having a volume, $V_{\rm coop}(z)$, that surrounds a point, x, y, z. The size of the region, $V_{\rm coop}(z)$, is such that it contains the characteristic critical free volume (v^*) . The relative free volume at z is related to $\rho_{\rm av}(z)$ by $(V_{\rm free}/V_{\rm hc})(z) = (\rho_{\rm hc}/\rho_{\rm av}(z)) - 1$, where $1/\rho_{\rm hc}$ = close-packed volume $V_{\rm hc}$ per mass.

Because the critical free volume, v^* , required for rearrangement is a constant, $V_{\rm coop}(z)$, and the cooperative length, $L_{\rm coop}(z)$, will change with density. At high density, the number (n^*) of cooperating particles and their surrounding volume, $V_{\rm coop}$, need to be large to sum to the total required v^* value, while at lower density, a smaller $V_{\rm coop}$ will contain the same v^* . Therefore, the CFV model predicts that $V_{\rm coop}(z)$ and $L_{\rm coop}(z)$ will decrease upon moving from the interior bulk toward the lower average densities near the free surface. This effect is shown diagrammatically in Figure 1a, where three cooperative regions at different locations near the surface have different $V_{\rm coop}$ but all contain the required critical amount of free space, v^* .

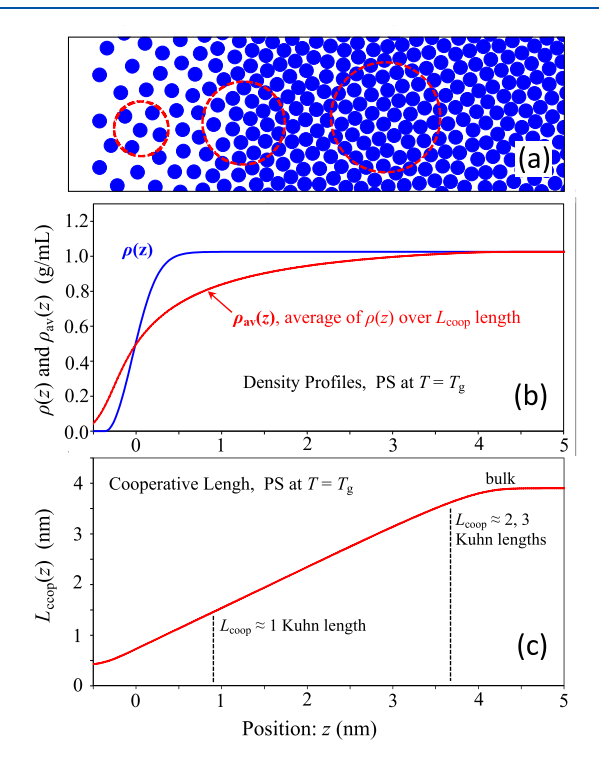


Figure 1. Local density, $\rho(z)$, average local density, $\rho_{\rm av}(z)$, and cooperative length, $L_{\rm coop}(z)$, as a function of position, z, across the polystyrene free surface. Middle panel, (b): $\rho(z)$ and $\rho_{\rm av}(z)$. Lower panel, (c): $L_{\rm coop}(z)$. $\rho(z)$ is calculated using the LCL EOS model, and $\rho_{\rm av}(z)$ and $L_{\rm coop}(z)$ follow from eq 4 (see text). The upper panel (c) is a diagrammatic representation of segments in a free surface region, where the segments inside the dashed circles comprise cooperatively rearranging groups. The group size, and thus the cooperative distance, changes with the location of the group because a smaller region can enclose the critical free volume (v^*) when it is near the regions of low local density near the surface.

Note that we do not assume that all the segments enclosed in $V_{\rm coop}$ must be cooperating; it could be just a subset, for example, a string-like collection that spans the region. Either way, we are assuming that $V_{\rm coop}$ encloses a region containing at least the required ν^* in free volume, although it may contain more if not all the segments within are required to cooperate. For this latter case, the amount of free volume enclosed in $V_{\rm coop}$ is assumed to be a constant and its value is proportional to ν^* . (The associated proportionality constant does not need to be evaluated in our procedure.)

In order to calculate $\rho_{\rm av}(z)$ and $(V_{\rm free}/V_{\rm hc})(z)$ for a particular material, in this case polystyrene, we must first calculate the local density profile $\rho(z)$. This is performed using the LCL EOS which, as noted above was fit to PS *PVT* data, combined with the square gradient approximation, $^{67-69}$ and data for the PS surface tension. Further details for these calculations are in the Supporting Information. The resulting local density profile $\rho(z)$ for PS (at $T=T_g$, P=1 atm) is shown as the blue curve in Figure 1b. As expected for polymer-free surfaces, 69 the density profile is sharp; the gradient in $\rho(z)$ is not much wider than 1 nm. The gradient in $\rho(z)$ remains sharp at other temperatures, for example, it broadens only slightly (only \sim 0.1 nm) at increased temperatures of 50–100° higher (see results in Supporting Information).

Calculation of $\rho_{\rm av}(z)$ also requires $V_{\rm coop}(z)$ and $L_{\rm coop}(z)$. We will approximate $L_{\rm coop}$ by calculating it at a single specific state point, corresponding to the conditions of bulk density at a chosen fixed T and P. This will allow us to solve for v^* , which is the required volume for a segmental motion, independent of the T and P at which it occurs. Note that the value of v^* cannot be resolved from the bulk dynamics alone because it is absorbed with other multiplicative constants in eqs 2 and 3. Here, we apply additional information on $L_{\rm coop}$ at bulk density that is obtainable from measurements of interfacial effects (see below), allowing for the constant v^* to be determined. We can then predict $L_{\rm coop}(z)$ at all other densities across the interface.

As observed above, $L_{\rm coop}$ must be on the scale of the characteristic intermolecular distances over which the caged segments cooperate with their surrounding near neighbors, next near neighbors, and so forth. Typical values are likely to be around 2 or 3 Kuhn lengths, and given the PS Kuhn length of 1.5 nm, 71 this implies an $L_{\rm coop}$ in the range of 3.0–4.5 nm.

We can verify that this is sensible using some independent experimental results. Dynamics data on polymer films show that the bulk-like region of the two layer (bulk, interfacial) model we have previously used disappears for films that are below 10 nm thick. 14 Therefore, a segment in the most buried section of a 10 nm thick film still behaves (in terms of alpha relaxation) like a bulk segment at that T and P. (Note that except for this most buried segment, essentially all other segments in the film do not experience bulk-like dynamics.) This segment in the most buried part of the film sits within a 10 nm/2 = 5.0 nm distance from the surface. It experiences a bulk-like density because it is evidently collecting sufficient free volume, over its cooperative distance, to yield a bulk relaxation time (i.e., $\rho(z)$ in eq 4 is bulk-like over its entire cooperative distance). Just beyond this cooperative distance, there will be a remaining outer portion (not "seen" by the interior segment) that will have a (nonbulk-like) changing local density with a gradient likely spanning approximately 1-2 nm, say 1.5 nm. (A 1–2 nm wide local density gradient is a reasonable value based on studies of free surfaces; ⁶⁹ see also note ref 72.) Putting this together implies that the bulk-like segment in the most buried

part of the film must have a cooperative distance of roughly $L_{\rm coop}\approx 3.5$ nm, that is, (5.0–1.5) nm. For PS, this translates to a value of 2.33 Kuhn lengths, which seems reasonable given the arguments noted above. For the purpose of further calculation, we will therefore take this 3.5 nm to be the value of $L_{\rm coop}$ in the bulk at a reference T,~P of 390 K, 1 atm, respectively. We believe that this $L_{\rm coop}$ value is sensible to within say, about $\pm 25\%$, and thus good for semiquantitative prediction. In future applications, if desired, its value could be fit to dynamics data to achieve even closer agreement.

At each position, z, $\rho_{\rm av}(z)$, and $V_{\rm coop}(z)$ [thus $L_{\rm coop}(z)$] can now be solved self-consistently based on the fixed value set for v^* . As noted above, we solved for v^* by knowing $L_{\rm coop}=3.5$ nm at the bulk density at T=390 K, P=1 atm. The approach involves simultaneously satisfying eq 4 together with the condition $v^*=[1-(\rho_{\rm av}(z)/\rho_{\rm hc})]V_{\rm coop}(z)$. Note that because the interface environment is non-isotropic, we use a rectangular-shaped averaging region (rather than a spherical shape). Starting with the bulk, $V_{\rm coop}=(2L_{\rm coop})^3$ is taken to be a symmetric cube, and then because the key direction (z) is normal to the surface, just the length $(2L_{\rm coop}(z))$ of the side in that direction changes on moving toward the surface.

Before moving to the Results section, we note that while here we model a dynamics enhancement due to the lowering of averaged density from the presence of a free interface, this approach is equally able to capture a slowdown in the dynamics. Increased relaxation times would be predicted by the CFV model for cases where there is an increase in density (decrease in free volume) relative to bulk over a small portion of the local density profile, an effect that has been observed, for example, in simulations. A possible cause would be a strong substrate—segment interaction.

4. RESULTS AND DISCUSSION

The results for $\rho_{\rm av}(z)$ and $L_{\rm coop}(z)$ as a function of position are shown in Figure 1b,c; these correspond to the PS melt at $T=T_{\rm g}$ (P=1 atm). We emphasize that in Figure 1b, the values for $\rho_{\rm av}(z)$ (red curve) depart significantly from those associated with the bulk density (blue curve), extending much further (over 4 nm) into the interior of the film, compared to $\rho(z)$ (blue curve). This difference is important because in bulk P-dependent dynamics, just small changes (e.g., 0.5%) in density at constant T can have a significant effect on τ . Turning to Figure 1c, the curve for $L_{\rm coop}(z)$ shows that the cooperative length is about 2 to 3 Kuhn lengths (\sim 4 nm) at the bulk-like interior of the sample (which, by the way, already occurs at around 4 nm in from the surface) but significantly decreases to about 1 Kuhn length (\sim 1.5 nm) when about 1 nm from the surface

We can compare some of the values for the cooperative length with results from other works. For example, in the free volume-based approach reported by Merabia and Long, 60,73 the length scale for several bulk polymers was found to be in the range of 3–5 nm near $T_{\rm g}$ which compares well with our bulk value of about ~ 4 nm. One contrast is that the cooperating group size in the Merabia et al. model $(N_{\rm c})$ goes roughly as $1/V_{\rm free}^{\ \ 2}$, while it would go as $1/V_{\rm free}$ for the CFV model (noting, of course, that $V_{\rm free}$ in each approach is not defined the same way). The results from the model reported by Salez et al. 49 (where cooperative groups are string-like) give a bulk cooperative length of about 5 or 6 nm near $T_{\rm g}$.

Following from the results for $\rho_{\rm av}(z)$, the average relative free volume, $(V_{\rm free}/V_{\rm hc})(z)=(\rho_{\rm hc}/\rho_{\rm av}(z))-1$, is shown as a

function of position in Figure 2a. Toward the interior, the departure from the bulk $V_{\rm free}/V_{\rm hc}$ levels off gradually, but the

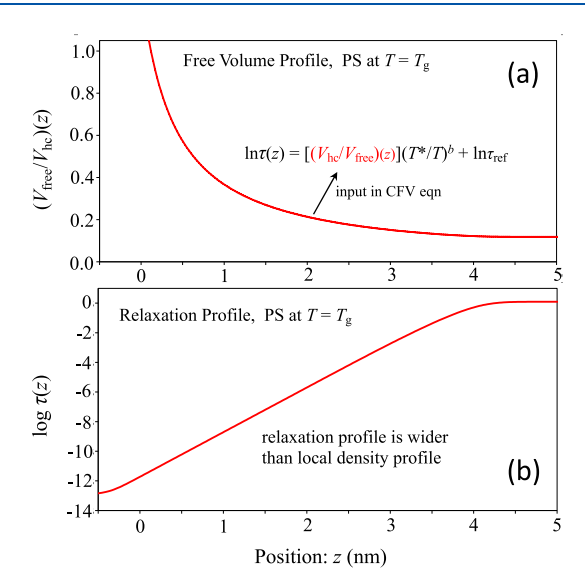


Figure 2. Local free volume, $(V_{\rm free}/V_{\rm hc})(z)$ [upper panel, (a)], and local relaxation time, $\tau(T,z)$ [lower panel, (b)], as a function of position, z, across polystyrene free surface. $(V_{\rm free}/V_{\rm hc})(z)$ is determined from $\rho_{\rm av}(z)$ (Figure 1b) and inputting $(V_{\rm free}/V_{\rm hc})(z)$ into eq 3 (fit to bulk polystyrene) leads to $\tau(T,z)$.

small differences from bulk that remain at 3 and 4 nm in still have a significant effect because dynamics on isotherms track with inverse free volume (ln $\tau \propto 1/V_{\rm free}$). Using $(V_{\rm free}/V_{\rm hc})(z)$ as the input in eq 3, we calculate relaxation times as a function of position, ln $\tau(T,z) = [(V_{\rm hc}/V_{\rm free})(z)](T^*/T)^b + \ln \tau_{\rm ref}$ based on the b, T^* , $\tau_{\rm ref}$ $V_{\rm hc}$ parameters that were determined from PS bulk dynamics and PVT data above. The resulting relaxation profile is shown in Figure 2b for the PS melt at $T=T_{\rm g}$. We have defined the dynamic $T_{\rm g}$ at $\tau=1$ s, which corresponds to $T_{\rm g}=365$ K; see note at ref 74. The model prediction is that relaxation times will increase by about 12 orders of magnitude on going from the free surface into the bulk interior, ultimately plateauing at about a little over 4 nm from the free surface. More discussion comparing relaxation and density profiles is further below.

The Figure 2 results are for PS at its glass transition temperature. Figure 3 shows the results for PS $\tau(T,z)$ profiles at multiple temperatures, ranging from 455 K (bottom curve) to 285 K (top curve). These plots reveal several important features. One is that the relaxation time associated with the plateau region, which is to say the bulk relaxation time, decreases as expected with increasing T. Second, the position of the onset of the plateau region also shifts with T. Here, as T decreases, the edge of the plateau will move more deeply toward the interior of the sample. The reason for this is the increased bulk density at lowered T (at ambient pressure). As discussed above, CFV predicts that an increased bulk density will result in an increase in the bulk cooperative length, $L_{\rm coop}$ (based on the requirement that $V_{\rm coop}$ contains the critical v^*). This is relevant because the edge of the plateau (the start of the deviation in dynamics) marks a position that is a distance L_{coop} away from the position where the local density, $\rho(z)$, first starts to deviate from the bulk density value. Though the distance to the deviation in the $\rho(z)$ profile is slightly Tdependent, the increase in L_{coop} (from the increased bulk

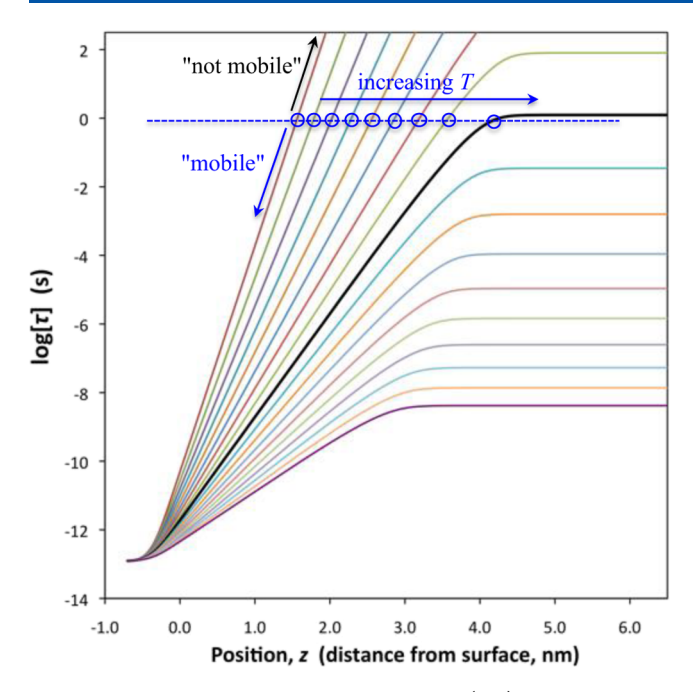


Figure 3. Polystyrene relaxation time profiles, $\tau(T,z)$, as a function of position, z, at multiple temperatures: 455 K (bottom curve) to 285 K (top curve) in increments of 10 K. The horizontal line is an isochronal cut at $\tau=1$ s; the position of intersection with any particular relaxation profile marks the boundary of mobile vs nonmobile segments for that temperature.

density) is stronger and therefore leads to the net shift in the location of the plateau edge, pushing it further in from the interface.

The results shown in Figure 3 allow us to make predictions for the mobile layer thickness. We define the cutoff for "mobile" vs "not mobile" at a relaxation time of $\tau = 1$ s (see note at ref 75); this is represented as a horizontal dashed line in the figure. The intersection points shift to a larger z, that is, a more interior position, as the sample temperature increases, which means that the mobile layer thickness increases. Figure 4 shows this quantity plotted against temperature. The CFV model predictions are in semiquantitative agreement with the corresponding experimental results for PS surfaces from the probe reorientation experiments by Paeng et al.;⁷⁶ the experiment and model both indicate a mobile layer thickness near $T = T_g$ of about 5 nm. (see note at ref 77.) The CFV definition, intended to mirror the experimental criterion, allows for only a rough comparison with some simulation results; for example, in the simulations of free standing films of beadspring polymers done by Shavit and Riggleman,⁷⁸ the mobile layers were defined to end where the plateau begins in the $\tau(z)$ profile (rather than isochronically), and so the mobile layer thickness decreased with increasing T. What is most important, however, is that their results and the CFV model (Figure 3) both illustrate the same qualitative behavior, in that the plateau moves up in τ value and further into the interior, as Tdecreases. (This means that if an isochronal criterion for mobile layer thickness was applied to the simulation results, the mobile layer thickness would increase with T in agreement with the CFV and experiment.)

As emphasized above, the reason density correlates with dynamics in the bulk is because it reflects the intermolecular environment that is relevant for cooperative intermolecular rearrangements. In a bulk sample, of course, the local density is

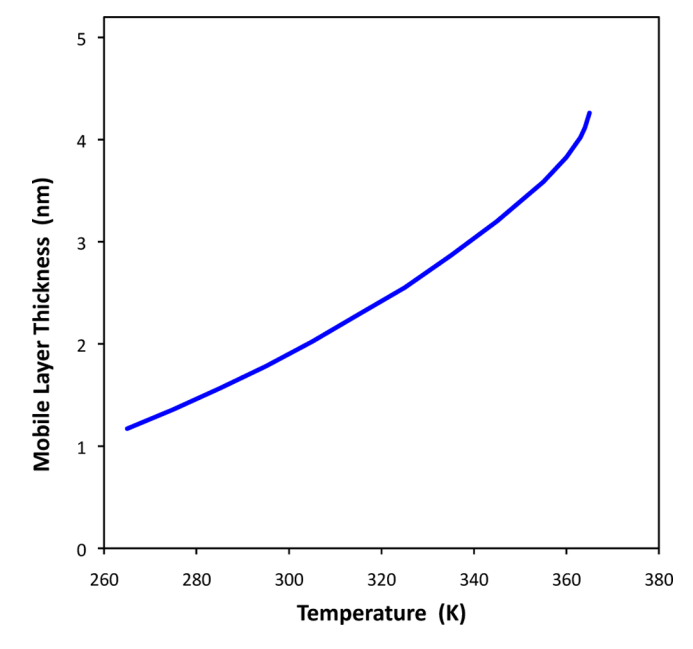


Figure 4. Polystyrene mobile layer thickness as a function of temperature. Mobile segments are defined as those segments having τ = 1 s or less; therefore, the value of the mobile layer thickness at each T comes from solving $\tau(T,z)$ for the position, z, where τ is equal to the cutoff value of 1 s.

independent of position. Near an interfacial region, it becomes important to account for how the density changes as a function of distance from the surface. However, as the CFV results presented here illuminate, it is not $\rho(z)$, the local density profile, that controls the dynamics near an interface because near a free surface, the $\rho(z)$ profile is extremely steep (e.g., ≈ 1 nm wide, while one Kuhn segment ≈ 1.5 nm). This means that although the value of $\rho(z)$ at some location could be relatively close to the bulk density, the average over a single near neighbor distance—relevant for considering the environmental contributions to cooperative segmental relaxation—could be closer to half of that. As the work here shows, using an averaged local density, $\rho_{\rm av}(z)$ better reflects the intermolecular environment

The CFV model results both connect with, and allow for a deeper understanding of, the simulation results that have accrued for dynamics at interfaces. $^{5-7,42,78-83}$ Both show that the gradient in the relaxation profile, $\tau(z)$, is several times wider than the gradient in the local density, $\rho(z)$. Using CFV, we conclude that the effect on $\tau(z)$ from the interface penetrates deeper into the interior because the relevant density for dynamics must account for cooperative distances that are on an intermolecular scale. Indeed, both the model and simulation show that as T decreases, the relaxation profiles get wider, while the local density profiles get even narrower. The shape of the model and simulated relaxation profiles are qualitatively similar.

We have noted previously, and reiterate here, that density (free volume) and segmental relaxation are closely linked. However, an important insight from the CFV model results here is that $\tau(z)$ is not simply the shape of $\rho(z)$ shifted further in. Our results show that the broad dynamic relaxation profile differs from the much sharper local density profile because the cooperative distance, $L_{\rm coop}(z)$, that is, the length scale over which local density contributes to form the average density, is position-dependent. The position-dependent averages translate

to wider relaxation profiles and mobile layer broadening, in agreement with the simulation and experiment.

Finally, the CFV model predicts that as T decreases, the sensitivity of the dynamics to the presence of an interface increases (larger deviation in τ from bulk). This is in satisfying agreement with experiment and simulation, however, the model goes further. It illuminates that this effect is rooted in the multiplicative coupling of the general form, $\tau(T,V) \propto \exp[f(T) \times g(V)]$, where a given density shift has a greater effect at lower T because f(T) is increasing.

ASSOCIATED CONTENT

Supporting Information

The Supporting Information is available free of charge at https://pubs.acs.org/doi/10.1021/acs.macromol.0c02742.

Details on LCL EOS analysis of bulk PS PVT data and density profile analysis from PS surface tension data, and details on CFV model analysis of bulk PS P-dependent dynamics data and P-dependent $T_{\rm g}$ from PVT data (PDF)

AUTHOR INFORMATION

Corresponding Author

Jane E. G. Lipson — Department of Chemistry, Dartmouth College, Hanover, New Hampshire 03755, United States; orcid.org/0000-0002-0177-9373; Email: jlipson@dartmouth.edu

Author

Ronald P. White – Department of Chemistry, Dartmouth College, Hanover, New Hampshire 03755, United States

Complete contact information is available at: https://pubs.acs.org/10.1021/acs.macromol.0c02742

Notes

The authors declare no competing financial interest.

■ ACKNOWLEDGMENTS

We gratefully acknowledge the financial support provided by the National Science Foundation (DMR-1708542 and DMR-2006504).

REFERENCES

- (1) Napolitano, S.; Glynos, E.; Tito, N. B. Glass Transition of Polymers in Bulk, Confined Geometries, and near Interfaces. *Rep. Prog. Phys.* **2017**, *80*, 036602.
- (2) Ediger, M. D.; Forrest, J. A. Dynamics near Free Surfaces and the Glass Transition in Thin Polymer Films: A View to the Future. *Macromolecules* **2014**, *47*, 471–478.
- (3) Richert, R. Dynamics of Nanoconfined Supercooled Liquids. *Annu. Rev. Phys. Chem.* **2011**, *62*, 65–84.
- (4) Alcoutlabi, M.; McKenna, G. B. Effects of Confinement on Material Behaviour at the Nanometre Size Scale. *J. Phys. Condens. Matter* **2005**, *17*, R461–R524.
- (5) Simmons, D. S. An Emerging Unified View of Dynamic Interphases in Polymers. *Macromol. Chem. Phys.* **2016**, 217, 137–148.
- (6) Schweizer, K. S.; Simmons, D. S. Progress towards a Phenomenological Picture and Theoretical Understanding of Glassy Dynamics and Vitrification near Interfaces and under Nanoconfinement. J. Chem. Phys. 2019, 151, 240901.
- (7) Baschnagel, J.; Varnik, F. Computer Simulations of Supercooled Polymer Melts in the Bulk and In-Confined Geometry. *J. Phys. Condens. Matter* **2005**, *17*, R851–R953.

- (8) Cangialosi, D.; Alegria, A.; Colmenero, J. Effect of Nanostructure on the Thermal Glass Transition and Physical Aging in Polymer Materials. *Prog. Polym. Sci.* **2016**, 54–55, 128–147.
- (9) Boucher, V. M.; Cangialosi, D.; Yin, H.; Schönhals, A.; Alegría, A.; Colmenero, J. T-g Depression and Invariant Segmental Dynamics in Polystyrene Thin Films. *Soft Matter* **2012**, *8*, 5119–5122.
- (10) Fukao, K.; Miyamoto, Y. Glass Transitions and Dynamics in Thin Polymer Films: Dielectric Relaxation of Thin Films of Polystyrene. *Phys. Rev. E: Stat. Phys., Plasmas, Fluids, Relat. Interdiscip. Top.* **2000**, *61*, 1743–1754.
- (11) Priestley, R. D.; Cangialosi, D.; Napolitano, S. On the Equivalence between the Thermodynamic and Dynamic Measurements of the Glass Transition in Confined Polymers. *J. Non-Cryst. Solids* **2015**, *407*, 288–295.
- (12) Kremer, F.; Tress, M.; Mapesa, E. U. Glassy Dynamics and Glass Transition in Nanometric Layers and Films: A Silver Lining on the Horizon. *J. Non-Cryst. Solids* **2015**, 407, 277–283.
- (13) White, R. P.; Lipson, J. E. G. Connecting Pressure-Dependent Dynamics to Dynamics under Confinement: The Cooperative Free Volume Model Applied to Poly(4-Chlorostyrene) Bulk and Thin Films. *Macromolecules* **2018**, *51*, 7924–7941.
- (14) Debot, A.; White, R. P.; Lipson, J. E. G.; Napolitano, S. Experimental Test of the Cooperative Free Volume Rate Model under 1D Confinement: The Interplay of Free Volume, Temperature, and Polymer Film Thickness in Driving Segmental Mobility. *ACS Macro Lett.* **2019**, *8*, 41–45.
- (15) White, R. P.; Lipson, J. E. G. To Understand Film Dynamics Look to the Bulk. *Phys. Rev. Lett.* **2020**, *125*, 058002.
- (16) White, R. P.; Lipson, J. E. G. The Cooperative Free Volume Rate Model for Segmental Dynamics: Application to Glass-Forming Liquids and Connections with the Density Scaling Approach. *Eur. Phys. J. E* **2019**, 42, 100.
- (17) White, R. P.; Lipson, J. E. G. Explaining the T,V-Dependent Dynamics of Glass Forming Liquids: The Cooperative Free Volume Model Tested against New Simulation Results. *J. Chem. Phys.* **2017**, 147, 184503.
- (18) White, R. P.; Lipson, J. E. G. Pressure-Dependent Dynamics of Polymer Melts from Arrhenius to Non-Arrhenius: The Cooperative Free Volume Rate Equation Tested against Simulation Data. *Macromolecules* **2018**, *51*, 4896–4909.
- (19) Roland, C. M.; Hensel-Bielowka, S.; Paluch, M.; Casalini, R. Supercooled Dynamics of Glass-Forming Liquids and Polymers under Hydrostatic Pressure. *Rep. Prog. Phys.* **2005**, *68*, 1405–1478.
- (20) Floudas, G.; Paluch, M.; Grzybowski, A.; Ngai, K. Molecular Dynamics of Glass-Forming Systems-Effects of Pressure; Springer: Berlin, 2011.
- (21) Casalini, R.; Mohanty, U.; Roland, C. M. Thermodynamic Interpretation of the Scaling of the Dynamics of Supercooled Liquids. *J. Chem. Phys.* **2006**, *125*, 014505.
- (22) Casalini, R.; Roland, C. M. An Equation for the Description of Volume and Temperature Dependences of the Dynamics of Supercooled Liquids and Polymer Melts. *J. Non-Cryst. Solids* **2007**, 353, 3936–3939.
- (23) Grzybowski, A.; Paluch, M. Universality of Density Scaling. In *The Scaling of Relaxation Processes*; Kremer, F., Loidl, A., Eds.; *Advances in Dielectrics*; Springer International Publishing: Cham, 2018, pp 77–119.
- (24) Dyre, J. C. Hidden Scale Invariance in Condensed Matter. J. Phys. Chem. B 2014, 118, 10007–10024.
- (25) Gnan, N.; Schrøder, T. B.; Pedersen, U. R.; Bailey, N. P.; Dyre, J. C. Pressure-Energy Correlations in Liquids. IV. "Isomorphs" in Liquid Phase Diagrams. *J. Chem. Phys.* **2009**, *131*, 234504.
- (26) Kipnusu, W. K.; Elsayed, M.; Kossack, W.; Pawlus, S.; Adrjanowicz, K.; Tress, M.; Mapesa, E. U.; Krause-Rehberg, R.; Kaminski, K.; Kremer, F. Confinement for More Space: A Larger Free Volume and Enhanced Glassy Dynamics of 2-Ethyl-1-Hexanol in Nanopores. J. Phys. Chem. Lett. 2015, 6, 3708—3712.
- (27) Kipnusu, W. K.; Elmahdy, M. M.; Elsayed, M.; Krause-Rehberg, R.; Kremer, F. Counterbalance between Surface and Confinement

- Effects As Studied for Amino-Terminated Poly(Propylene Glycol) Constraint in Silica Nanopores. *Macromolecules* **2019**, *52*, 1864–1873.
- (28) Debot, A.; Tripathi, P.; Napolitano, S. Solution Filtering Affects the Glassy Dynamics of Spincoated Thin Films of Poly(4-Chlorostyrene). *Eur. Phys. J. E* **2019**, 42, 102.
- (29) Panagopoulou, A.; Napolitano, S. Irreversible Adsorption Governs the Equilibration of Thin Polymer Films. *Phys. Rev. Lett.* **2017**, *119*, 097801.
- (30) Panagopoulou, A.; Rodríguez-Tinoco, C.; White, R. P.; Lipson, J. E. G.; Napolitano, S. Substrate Roughness Speeds Up Segmental Dynamics of Thin Polymer Films. *Phys. Rev. Lett.* **2020**, *124*, 027802.
- (31) Adrjanowicz, K.; Kaminski, K.; Koperwas, K.; Paluch, M. Negative Pressure Vitrification of the Isochorically Confined Liquid in Nanopores. *Phys. Rev. Lett.* **2015**, *115*, 265702.
- (32) Adrjanowicz, K.; Kaminski, K.; Tarnacka, M.; Szklarz, G.; Paluch, M. Predicting Nanoscale Dynamics of a Glass-Forming Liquid from Its Macroscopic Bulk Behavior and Vice Versa. *J. Phys. Chem. Lett.* **2017**, *8*, 696–702.
- (33) Tarnacka, M.; Kipnusu, W. K.; Kaminska, E.; Pawlus, S.; Kaminski, K.; Paluch, M. The Peculiar Behavior of the Molecular Dynamics of a Glass-Forming Liquid Confined in Native Porous Materials the Role of Negative Pressure. *Phys. Chem. Chem. Phys.* **2016**, *18*, 23709–23714.
- (34) Adrjanowicz, K.; Winkler, R.; Dzienia, A.; Paluch, M.; Napolitano, S. Connecting 1D and 2D Confined Polymer Dynamics to Its Bulk Behavior via Density Scaling. *ACS Macro Lett.* **2019**, *8*, 304–309.
- (35) Tarnacka, M.; Mierzwa, M.; Kamińska, E.; Kamiński, K.; Paluch, M. High-Pressure Experiments as a Novel Perspective to Study the Molecular Dynamics of Glass-Forming Materials Confined at the Nanoscale. *Nanoscale* **2020**, *12*, 10600–10608.
- (36) Simon, S. L.; Park, J.-Y.; McKenna, G. B. Enthalpy Recovery of a Glass-Forming Liquid Constrained in a Nanoporous Matrix: Negative Pressure Effects. *Eur. Phys. J. E* **2002**, *8*, 209–216.
- (37) Huang, X.; Roth, C. B. Changes in the Temperature-Dependent Specific Volume of Supported Polystyrene Films with Film Thickness. *J. Chem. Phys.* **2016**, *144*, 234903.
- (38) Unni, A. B.; Vignaud, G.; Chapel, J. P.; Giermanska, J.; Bal, J. K.; Delorme, N.; Beuvier, T.; Thomas, S.; Grohens, Y.; Gibaud, A. Probing the Density Variation of Confined Polymer Thin Films via Simple Model-Independent Nanoparticle Adsorption. *Macromolecules* 2017, 50, 1027–1036.
- (39) Napolitano, S. Irreversible Adsorption of Polymer Melts and Nanoconfinement Effects. *Soft Matter* **2020**, *16*, 5348–5365.
- (40) Napolitano, S.; Capponi, S.; Vanroy, B. Glassy Dynamics of Soft Matter under 1D Confinement: How Irreversible Adsorption Affects Molecular Packing, Mobility Gradients and Orientational Polarization in Thin Films. *Eur. Phys. J. E* **2013**, *36*, 61.
- (41) Napolitano, S.; Rotella, C.; Wübbenhorst, M. Can Thickness and Interfacial Interactions Univocally Determine the Behavior of Polymers Confined at the Nanoscale? *ACS Macro Lett.* **2012**, *1*, 1189–1193
- (42) Diaz-Vela, D.; Hung, J.-H.; Simmons, D. S. Temperature-Independent Rescaling of the Local Activation Barrier Drives Free Surface Nanoconfinement Effects on Segmental-Scale Translational Dynamics near Tg. ACS Macro Lett. 2018, 7, 1295–1301.
- (43) White, R. P.; Lipson, J. E. G. How Free Volume Does Influence the Dynamics of Glass Forming Liquids. *ACS Macro Lett.* **2017**, *6*, 529–534.
- (44) White, R. P.; Lipson, J. E. G. Cooperative Free Volume Rate Model Applied to the Pressure-Dependent Segmental Dynamics of Natural Rubber and Polyurea. *Rubber Chem. Technol.* **2019**, *92*, *612*–624.
- (45) Araujo, S.; Delpouve, N.; Domenek, S.; Guinault, A.; Golovchak, R.; Szatanik, R.; Ingram, A.; Fauchard, C.; Delbreilh, L.; Dargent, E. Cooperativity Scaling and Free Volume in Plasticized Polylactide. *Macromolecules* **2019**, *52*, 6107–6115.

- (46) Kipnusu, W. K.; Elsayed, M.; Iacob, C.; Pawlus, S.; Krause-Rehberg, R.; Paluch, M. Glassy Dynamics Predicted by Mutual Role of Free and Activation Volumes. *Soft Matter* **2019**, *15*, 4656–4661.
- (47) Long, D.; Lequeux, F. Heterogeneous Dynamics at the Glass Transition in van Der Waals Liquids, in the Bulk and in Thin Films. *Eur. Phys. J. E* **2001**, *4*, 371–387.
- (48) Merabia, S.; Sotta, P.; Long, D. Heterogeneous Nature of the Dynamics and Glass Transition in Thin Polymer Films. *Eur. Phys. J. E* **2004**, *15*, 189–210.
- (49) Salez, T.; Salez, J.; Dalnoki-Veress, K.; Raphaël, E.; Forrest, J. A. Cooperative Strings and Glassy Interfaces. *Proc. Natl. Acad. Sci. U.S.A.* **2015**, *112*, 8227–8231.
- (50) Phan, A. D.; Schweizer, K. S. Dynamic Gradients, Mobile Layers, T-g Shifts, Role of Vitrification Criterion, and Inhomogeneous Decoupling in Free-Standing Polymer Films. *Macromolecules* **2018**, *51*, 6063–6075.
- (51) Lipson, J. E. G.; Milner, S. T. Percolation Model of Interfacial Effects in Polymeric Glasses. *Eur. Phys. J. B* **2009**, *72*, 133–137.
- (52) Mirigian, S.; Schweizer, K. S. Dynamical Theory of Segmental Relaxation and Emergent Elasticity in Supercooled Polymer Melts. *Macromolecules* **2015**, *48*, 1901–1913.
- (53) Arutkin, M.; Raphael, E.; Forrest, J. A.; Salez, T. Cooperative Strings and Glassy Dynamics in Various Confined Geometries. *Phys. Rev. E* **2020**, *101*, 032122.
- (54) Vogel, H. The Temperature Dependence Law of the Viscosity of Fluids. *Phys. Z.* **1921**, 22, 645–646.
- (55) Fulcher, G. S. Analysis of Recent Measurements of the Viscosity of Glasses. J. Am. Ceram. Soc. 1925, 8, 339-355.
- (56) Tammann, G.; Hesse, W. The Dependancy of Viscosity on Temperature in Hypothermic Liquids. Z. Anorg. Allg. Chem. 1926, 156, 245.
- (57) Cohen, M. H.; Turnbull, D. Molecular Transport in Liquids and Glasses. J. Chem. Phys. 1959, 31, 1164–1169.
- (58) Williams, M. L.; Landel, R. F.; Ferry, J. D. The Temperature Dependence of Relaxation Mechanisms in Amorphous Polymers and Other Glass-forming Liquids. *J. Am. Chem. Soc.* **1955**, *77*, 3701–3707.
- (59) Doolittle, A. K. Studies in Newtonian Flow .2. the Dependence of the Viscosity of Liquids on Free-Space. *J. Appl. Phys.* **1951**, 22, 1471–1475.
- (60) Merabia, S.; Long, D. Heterogeneous Dynamics at the Glass Transition in van Der Waals Liquids: Determination of the Characteristic Scale. *Eur. Phys. J. E* **2002**, *9*, 195–206.
- (61) Merabia, S.; Long, D. Heterogeneous Dynamics and Pressure Dependence of the Dynamics in van Der Waals Liquids. *Macromolecules* **2008**, *41*, 3284–3296.
- (62) Chen, K.; Saltzman, E. J.; Schweizer, K. S. Segmental Dynamics in Polymers: From Cold Melts to Ageing and Stressed Glasses. *J. Phys. Condens. Matter* **2009**, *21*, 503101.
- (63) White, R. P.; Lipson, J. E. G. Polymer Free Volume and Its Connection to the Glass Transition. *Macromolecules* **2016**, 49, 3987–4007
- (64) Lipson, J. E. G.; White, R. P. Connecting Theory and Experiment To Understand Miscibility in Polymer and Small Molecule Mixtures. *J. Chem. Eng. Data* **2014**, *59*, 3289–3300.
- (65) Zoller, P.; Walsh, D. Standard Pressure-Volume-Temperature Data for Polymers; Technomic Pub Co.: Lancaster, PA, 1995.
- (66) Schwartz, G. A.; Colmenero, J.; Alegría, Á. Dielectric Study of the Segmental Relaxation of Low and High Molecular Weight Polystyrenes under Hydrostatic Pressure. *J. Non-Cryst. Solids* **2007**, 353, 4298–4302.
- (67) Sanchez, I. C. Physics of Polymer Surfaces and Interfaces; Butterworth: Greenwich, CT, 1992.
- (68) Poser, C. I.; Sanchez, I. C. Surface-Tension Theory of Pure Liquids and Polymer Melts. *J. Colloid Interface Sci.* **1979**, 69, 539–548
- (69) Dee, G. T.; Sauer, B. B. The Surface Tension of Polymer Liquids. *Adv. Phys.* **1998**, 47, 161–205.

- (70) Wu, S. Surface and Interfacial Tensions of Polymer Melts .2. Poly(Methyl Methacrylate), Poly(Normal-Butyl Methacrylate), and Polystyrene. *J. Phys. Chem.* **1970**, *74*, 632.
- (71) Lodge, T. P.; McLeish, T. C. B. Self-Concentrations and Effective Glass Transition Temperatures in Polymer Blends. *Macromolecules* **2000**, *33*, 5278–5284.
- (72) We assume this gradient width range is also reasonable at substrate surfaces such as the experimentally studied systems we connected with (Al-capped poly 4-chlorostyrene films) in ref 14.
- (73) Merabia, S.; Long, D. Heterogeneous Dynamics, Ageing, and Rejuvenating in van Der Waals Liquids. *J. Chem. Phys.* **2006**, *125*, 234901.
- (74) This choice of dynamic $T_{\rm g}$ is a compromise that matches the ref 66 bulk dynamics data (used in characterizing the model) closer to common calorimetric $T_{\rm g}$ measurements for PS. Choosing for example a dynamic $T_{\rm g}$ at $\tau=100$ s would not change any of the main conclusions here.
- (75) Other choices of cutoff, for example at $\tau = 10$ s, 100 s, and so forth can be implemented and do not affect the conclusions; see note at ref 74.
- (76) Paeng, K.; Swallen, S. F.; Ediger, M. D. Direct Measurement of Molecular Motion in Freestanding Polystyrene Thin Films. *J. Am. Chem. Soc.* **2011**, *133*, 8444–8447.
- (77) The results compared here connect with segmental dynamics (α relaxation) and are not expected to directly correspond to confinement effects on pseudothermodynamic $T_{\rm g}$ which can act on larger length scales; for example see refs 1,9–12.
- (78) Shavit, A.; Riggleman, R. A. Physical Aging, the Local Dynamics of Glass-Forming Polymers under Nanoscale Confinement. *J. Phys. Chem. B* **2014**, *118*, 9096–9103.
- (79) Hanakata, P. Z.; Douglas, J. F.; Starr, F. W. Local Variation of Fragility and Glass Transition Temperature of Ultra-Thin Supported Polymer Films. *J. Chem. Phys.* **2012**, *137*, 244901.
- (80) Hanakata, P. Z.; Betancourt, B. A. P.; Douglas, J. F.; Starr, F. W. A Unifying Framework to Quantify the Effects of Substrate Interactions, Stiffness, and Roughness on the Dynamics of Thin Supported Polymer Films. *J. Chem. Phys.* **2015**, *142*, 234907.
- (81) Sussman, D. M.; Schoenholz, S. S.; Cubuk, E. D.; Liu, A. J. Disconnecting Structure and Dynamics in Glassy Thin Films. *Proc. Natl. Acad. Sci. U.S.A.* **2017**, *114*, 10601–10605.
- (82) Lang, R. J.; Simmons, D. S. Interfacial Dynamic Length Scales in the Glass Transition of a Model Freestanding Polymer Film and Their Connection to Cooperative Motion. *Macromolecules* **2013**, *46*, 9818–9825.
- (83) Shavit, A.; Riggleman, R. A. Influence of Backbone Rigidity on Nanoscale Confinement Effects in Model Glass-Forming Polymers. *Macromolecules* **2013**, *46*, 5044–5052.